†Acknowledgment is made to the donors of The Petroleum Research Fund, administered by the American Chemical Society, for partial support of this research.

[1]L. M. Mataresse and C. Kikuchi, J. Chem. Phys. 33, 601 (1060); see also L. M. Mataresse, J. Chem. Phys. 34, 336 (1961), who has also observed some of the forbidden transitions.

[2]S. A. Marshall and A. R. Reinberg, Phys. Rev. 132, 134 (1963).

[3]W. Low, in *Solid State Physics*, Suppl. 2, edited by F. Seitz and D. Turnbull (Academic, New York, 1960).

[4]J. L. Prather, *Atomic Energy Levels in Crystals*, Natl. Bur. Std. Monograph No. 19 (U. S. Government Printing Office, Washington, D. C., 1961).

[5]M. T. Hutchings, in *Solid State Physics*, edited by F. Seitz and D. Turnbull (Academic, New York, 1964), Chap. XVI.

[6]F. R. Hurd, M. Sachs, and W. O. Hershberger, Phys. Rev. 93, 373 (1954).

PHYSICAL REVIEW B VOLUME 2, Number 1 1 JULY 1870

Jahn-Teller Distortions of Ag^{2+} Ions in SrF_2 and CaF_2 by Odd Modes

R. C. Fedder

Department of Physics, University of Cincinnati, Cincinnati, Ohio 45221

(Received 14 August 1969; revised manuscript received 3 February 1970)

An anistropic EPR spectrum of Ag^{2+} ions has been observed at 4.2 °K in single crystals of CaF_2 and SrF_2 that have been doped with silver. X rays convert the silver from the Ag^{1+} to the Ag^{2+} state. The results may be fitted with spin Hamiltonians with $S=\frac{1}{2}$, $g_{\parallel}=1.997\pm0.001$ and $g_{\perp}=2.106\pm0.001$ for CaF_2, and $g_{\parallel}=1.988\pm0.001$ and $g_{\perp}=2.130\pm0.001$ for SrF_2. Hyperfine interactions with the silver nucleus are not resolved, but are expected to be small from symmetry considerations. Hyperfine interactions with two equivalent fluorines are observed and have the characteristic 1:2:1 intensity ratio with $A_{\parallel}=58.6\times10^{-4}$ cm^{-1} and $A_{\perp}=14.5\times10^{-4}$ cm^{-1} for CaF_2:Ag^{2+}, and $A_{\parallel}=30.6\times10^{-4}$ cm^{-1} and $A_{\perp}=14.6\times10^{-4}$ cm^{-1} for SrF_2:Ag^{2+}. Additional hyperfine structure from four other fluorine nuclei can be resolved when the magnetic field is along a ⟨110⟩ direction. Optical absorption bands are observed in the x-rayed CaF_2:Ag^{2+} at 25 550 and 19 000 cm^{-1}. One of the optical absorption bands and the g shift can be correlated by assuming that the Ag^{2+} excited state mixes with the fluorine ligands. This physical system is unusual in that the silver ions distort from cubic symmetry by moving off center in ⟨110⟩ directions away from the central position and should have an electric dipole moment. In the distorted position, the hole in the d shell of Ag^{2+} is shared with a pair of ⟨100⟩-oriented fluorine ions.

I. INTRODUCTION

Jahn-Teller effects[1] have been a subject of increasing attention recently. A considerable amount of theoretical effort has gone into the study of static and dynamic Jahn-Teller effects for the doublet (Γ_3^+) ground state. Bersuker,[2] Ham,[3] and O'Brien[4] have made important contributions beyond the earlier work of Opik, Pryce, and others.[5] Coffman[6] and Höchli[7] have recently found some experimental evidence for tunneling effects in the electron-paramagnetic-resonance (EPR) spectrum of Cu^{2+} in MgO and Sc^{2+} in CaF_2 and SrF_2.

Far less information is available on the distortions of triplet ground states, and the theory appears to be more complicated and less developed. Ham[3] has developed a theory of dynamical quenching of the orbital angular momentum to successfully explain the reduced g shifts of some paramagnetic ions that have triplet ground states. Both Ham[8] and Sturge[9] have recently reviewed the experimental and theoretical status of Jahn-Teller effects.

Relatively few examples of static Jahn-Teller effects have been observed for triplet states. One example is the work of Estle *et al.*[10] and Morigaki[11] who have attributed an anisotropic spectrum of Cr^{2+} to distortions along a line bisecting the angle to a nearest-neighbor pair of sulphurs in CdS. Similar spectra have been observed for Cr^{2+} in ZnSe, CaF_2, and CdF_2. A model related to the one presented in this paper may apply to the above-mentioned experiments. Recently, Ham[8] has reviewed the experimental situation for Jahn-Teller effects in orbital triplet states.

In this article, we will present results for the static distortions of the Ag^{2+} ion in CaF_2 and SrF_2,[12] where the ground electronic state is a Γ_5^+ triplet

orbital. The symmetry of the EPR spectrum indicates that the Ag^{2+} ion distorts from cubic symmetry to a symmetry C_{2v} by an odd mode of distortion. In the distorted position, the hole in the d shell is shared mainly with a pair of fluorines. We will show that the EPR spectrum has a natural relationship to the V_K center of Känzig[13] as explored for CaF_2 in the work of Hayes and Twidell[14] and Sierro.[15] In the following paper, we will develop a microscopic model for the Jahn-Teller distortions. EPR studies have also been carried out for Ag^{2+} and Cu^{2+} ions in CdF_2 [12] but the results are somewhat different and will be discussed in a separate publication.

II. EXPERIMENTAL PROCEDURES

A. Sample Preparation

The samples were prepared by diffusing silver into crystals of CaF_2 and SrF_2 purchased from Optovac and the Harshaw Chemical Co. First the crystals were x-ray oriented and cut to an approximate size of $0.1\times0.1\times\frac{1}{2}$ in. A thin film of silver was then deposited on all sides of the crystal by vacuum evaporation from a tantalum boat.

The crystals were then placed in a quartz tube with argon gas flowing over the sample and heated to 900 °C for 12–15 h. Without delay the crystals were removed from the oven to cool and then mounted in the x-band cavity to observe the EPR signal. A dull gray color extended through the otherwise transparent crystals. Crystals prepared in this way have a complicated EPR spectrum, but no part of the spectrum can be identified with Ag^{2+} in cubic coordination or with Jahn-Teller distortions from the cubic configuration. Very little effort was devoted to the analysis of this complex spectrum.

After the crystals were x rayed at room temperature the spectrum of Ag^{2+} ions appeared and was analyzed in detail. Other complex spectra are also present after x raying but are not analyzed. Our crystals were x irradiated in a GE x-ray unit with 70 kV applied to the tube at a current of 6 mA. Two opposite faces of the crystal were exposed at room temperature for 15–20 min on each face. After the exposure, the crystals have a purple color and a part of the spectrum can be identified as Ag^{2+}. Silver ions are apparently converted from the monovalent to the divalent state by the x rays.

B. EPR Spectrometer and Stressing Arrangement

Our EPR spectrometer has a 30-mc superheterodyne detection system with phase-locked automatic frequency control (AFC) for both the primary klystron and the local oscillator. The primary klystron is stabilized against the 42nd harmonic of a stable uhf source that can be tuned from 221 to 223 mc. The local oscillator is locked 30 mc to either side of the primary klystron frequency. A 30-mc reference frequency for phase detection is brought out of the 30-mc AFC amplifier in the local oscillator stabilization loop. Absorption signals may be plotted directly by recording the output of the 30-mc phase detector.

The cylindrical cavity operates in the TE_{011} mode with the sample placed in the strong microwave field at the center of the cavity. Stress can be applied to the sample by applying force to a stainless-steel rod that rests on the top end of the sample. The bottom end of the sample is supported by a heavy plate that is rigidly connected to the waveguide. With this arrangement stress can be applied along the axis of the cylindrical cavity, that is in the same direction as the microwave field. The external magnetic field is applied perpendicular to the direction of stress and can be rotated about this axis. Difficulties with bubbling helium have been eliminated by housing the cavity in an evacuated box.

III. EXPERIMENTAL DISCUSSION AND RESULTS

After the crystals are x rayed in the manner previously described an anisotropic EPR spectrum appears and is assigned to the Ag^{2+} ion. X raying of the crystal apparently converts the silver ion from the monovalent to the divalent state. The fluorite crystal structure has a basis consisting of a face-centered-cubic (fcc) lattice of cations with origin at (0, 0, 0) and two fcc lattices of fluorines centered at $(\frac{1}{4}, \frac{1}{4}, \frac{1}{4})$ and $(\frac{3}{4}, \frac{3}{4}, \frac{3}{4})$. An Ag^{2+} ion substituting for the cation will then be surrounded by eight fluorine ions. Our experimental results and analysis indicate that after x raying the Ag^{2+} ion is surrounded by eight fluorine ions and must therefore be in either the interstitial or substitutional position. Charge compensation considerations and also our stress measurements lead us to

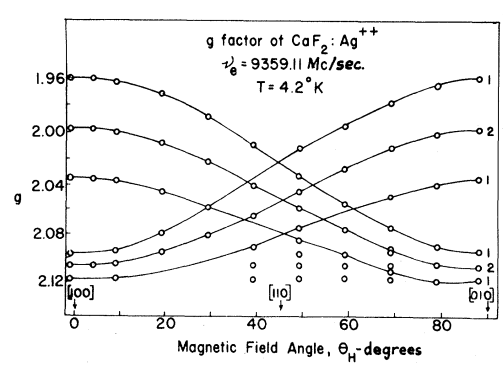

FIG. 1. Variation of the g values for CaF_2:Ag^{2+} versus the angular orientation of the magnetic field in a {100} plane.

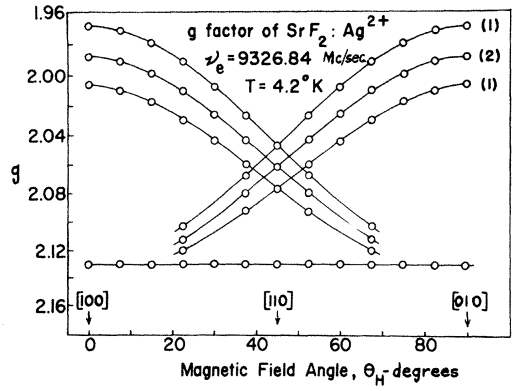

FIG. 2. Variation of g values with magnetic field orientation for SrF_2:Ag^{2+}.

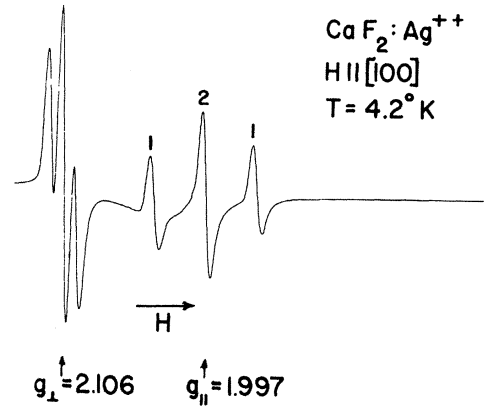

FIG. 3. Electron-paramagnetic-resonance spectrum of CaF_2:Ag^{2+} when the field is oriented along a ⟨100⟩ direction.

the conclusion that the substitutional position is more likely.

Three sets of lines appear in the EPR spectra of Ag^{2+} in CaF_2 and SrF_2 at 4.2 °K as shown in Figs. 1 and 2. Each set of lines consists of three hyperfine lines having a 1:2:1 intensity ratio for all orientations of the magnetic field. This behavior is characteristic of a hyperfine interaction with a pair of equivalent fluorines. Figure 3 shows a typical spectrum for CaF_2: Ag^{2+} when the field is along a ⟨100⟩ direction. Two of the three sets of lines overlap at $g_\perp = 2.106$ to produce twice the intensity of the high-field line. The g tensors have cylindrical symmetry about ⟨100⟩ directions.

When the field is parallel to a ⟨110⟩ direction the hyperfine interaction with four other equivalent fluorines can be resolved as shown in Fig. 4. The splitting between these lines is 2.8 G or also about 2.8×10^{-4} cm^{-1}. This resolution can only be obtained for the low-field line. No hyperfine interaction with the silver nucleus is observed, but later we shall see that the wave function has a null at the silver nucleus so that no hyperfine interaction is expected.

The magnetic resonance spectrum of any one of the three sets of resonance lines can be described by the following spin Hamiltonian:

$$\begin{aligned} H = {} & g_\parallel \beta H_z S_z + g_\perp \beta (H_x S_x + H_y S_y) + A_\parallel (I_{1z} + I_{2z}) S_z \\ & + A_\perp [(I_{1x} + I_{2x}) S_x + (I_{1y} + I_{2y}) S_y] + a_3 \vec{I}' \cdot \vec{S} \\ & + d_3 \{ 3[(I_{3y} + I_{4y}) S_y + (I_{5x} + I_{6x}) S_x] - \vec{I}' \cdot \vec{S} \} , \qquad (1) \end{aligned}$$

where $\vec{I}' = \vec{I}_3 + \vec{I}_4 + \vec{I}_5 + \vec{I}_6$.

The parameters a_3 and d_3 of the last term cannot be fully determined since the splitting can only be resolved when the field is along a ⟨110⟩ direction. Table I gives the values of the parameters for Ag^{2+} in SrF_2 and CaF_2. $g_\parallel$ is the g factor as measured along a ⟨100⟩ direction. There are three sets of g ellipsoids with $g_\parallel$ along the three possible ⟨100⟩ directions and with each ellipsoid having cylindrical symmetry about a ⟨100⟩ axis.

We have applied uniaxial stress to the CaF_2: Ag^{2+} crystal along a ⟨001⟩ direction with the magnetic field along a ⟨110⟩ direction. As shown in Fig. 5 the intensity of the low-field line increases as the stress is increased. This can also be plotted in terms of the energy separation of the vibronic states in different potential wells as in Fig. 6. The position of the vibronic energy levels initially changes linearly with stress but finally becomes nonlinear at higher stresses. Initially the slope is 315 cm^2 sec^{-1}/dyn. It is important to note that at sufficiently low temperatures the random strains would cause the intensity of the lines to remain unaffected until the externally applied strain became of the order of the random strain fields. Since the intensity changes immediately even at 1.5 °K and with small stresses, we conclude that random strains are not important. We observed that the intensity of the lines changed quickly in less than 1

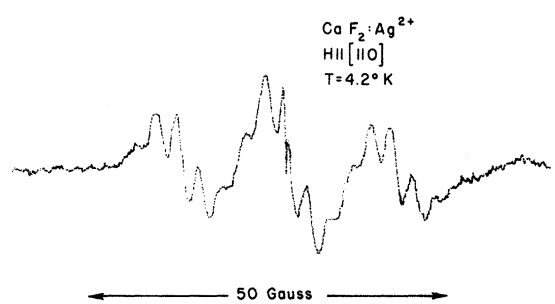

FIG. 4. Additional hyperfine structure on the low-field line when the field has a ⟨110⟩ orientation (CaF_2: Ag^{2+}).

TABLE I. Measured values of various parameters for Ag^{2+} ions in SrF_2 and CaF_2.

	$g_{\parallel}$	$g_{\perp}$	$A_{\parallel}(10^{-4}\ cm^{-1})$	$A_{\perp}(10^{-4}\ cm^{-1})$	Optical absorption (cm^{-1})
$CaF_2:Ag^{2+}$	1.997 ± 0.001	2.106 ± 0.001	58.6	14.5	19 000, 25 550
$SrF_2:Ag^{2+}$	1.988 ± 0.001	2.130 ± 0.001	30.6	14.6	...

sec when the stress was applied. If the spectra were due to charge compensated Ag^{2+} in interstitial positions, it is likely that the reorientation rate would be much slower than 1 sec. Any defect near the Ag^{2+} ion would tend to "lock-in" one orientation.

EPR spectra were also taken at liquid-hydrogen temperatures and it is observed that the lines broaden without shifting. At liquid-nitrogen temperatures the spectra are not observable. A motionally averaged sharp line does not appear at higher temperatures as often happens in many EPR experiments where distortions are involved. Rather the lines broaden out and become unobservable. We have not tried to carry out systematic linewidth and relaxation time measurements as a function of temperature.

Another bit of data is available in the form of optical absorptions observed at 25 550 and 19 000 cm^{-1} in the x-rayed material. Absorptions were observed at room temperature and liquid-nitrogen temperatures as shown in Fig. 7. Such absorptions are not observed in the un-x-rayed material or in undoped and un-x-rayed material. We searched for absorption in the infrared but nothing of significance was found. Table I summarizes the data for CaF_2 and SrF_2.

Our interpretation of these data will be in terms of Jahn-Teller distortions of the triplet electronic state of the Ag^{2+} ion. The hyperfine structure on the fluorines hints that the spectrum has a relationship to the F_2^- molecular ion which was first explored in detail by Castner and Känzig.[16] Indeed, in our model the hole in the $4d$ shell of the silver spreads out to the surrounding fluorines. An odd mode of distortion coupling between fluorine hole states causes the Ag^{2+} ion to move toward a pair of fluorines. In this distorted position the hole on the central ion is shared with the F_2^- molecular ion.

IV. MAGNETIC RESONANCE ANALYSIS

A. Wave Function and g Factor

In Sec. III, we expressed the experimental results in terms of a spin Hamiltonian. From this Hamiltonian we infer that the ground-state wave function of the Ag^{2+} ion has some of the F_2^- wave function mixed in to give the observed hyperfine structure. It is also likely that crystal fields, resulting from the distortion, will mix in some p state of the central silver ion. The ground-state wave function may be written as

$$|\Gamma_4\rangle = \alpha_4 (\sqrt{\tfrac{3}{2}})(xz+yz) + \beta_4 z + \gamma_4\left(\frac{z_1+z_2}{\sqrt{2}}\right) + \delta_4\left(\frac{s_1-s_2}{\sqrt{2}}\right), \quad (2)$$

which is a state of zero angular momentum and transforms as Γ_4 under C_{2v}.[17] The first two terms come from the d and p orbitals of the central ion while the third and fourth terms represent the covalent coupling to the fluorines. Couplings to fluorines 3, 4, 5, and 6 have not been included, although they are observed in the experiment. The ground-state wave function is pictured in

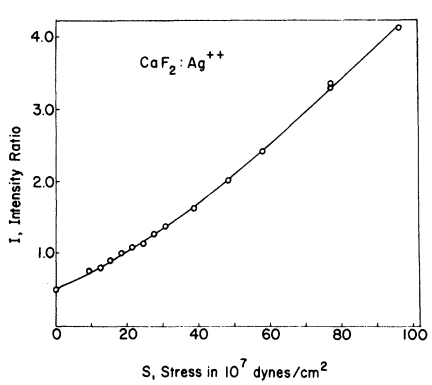

FIG. 5. Variation of the relative intensities of the resonance lines as a function of the stress along a ⟨001⟩ direction. The magnetic field is along a ⟨110⟩ direction.

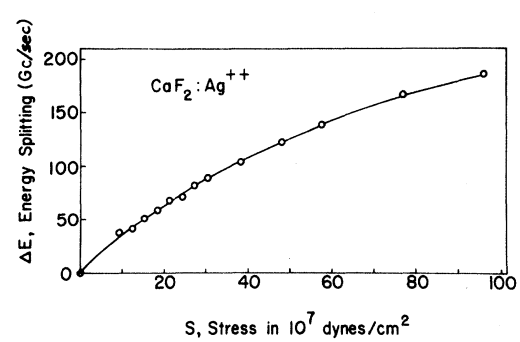

FIG. 6. Plot of the energy separation between the ground vibronic states of different potential wells as a function of the external stress applied along a ⟨001⟩ direction. These energy splittings are deduced from the data of Fig. 5.

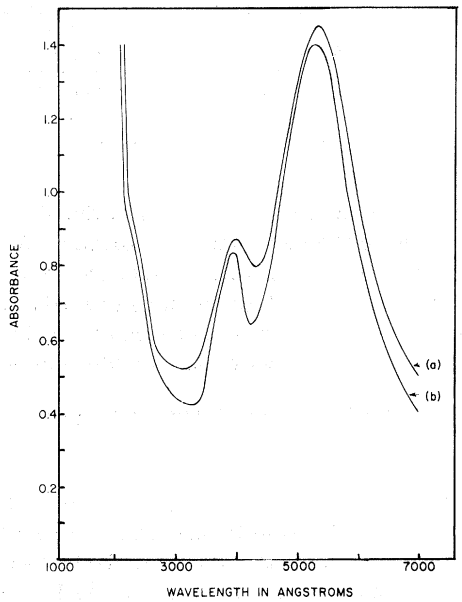

FIG. 7. Optical absorption in CaF_2:Ag^{2+} as observed at (a) room temperature and (b) liquid-nitrogen temperature.

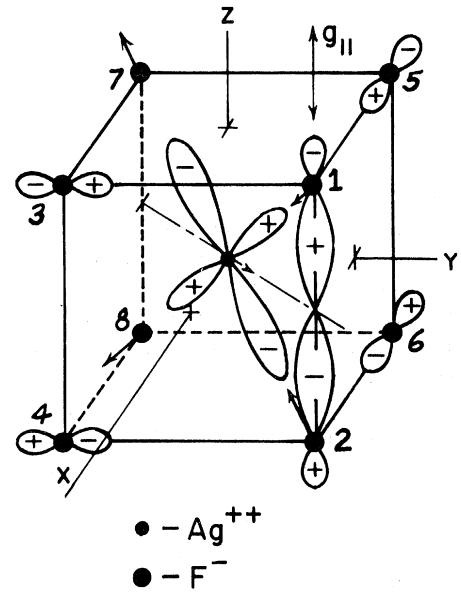

FIG. 8. Pictorial representation of the ground-state wave function for the distorted configuration.

Fig. 8.

Since we are dealing with a singlet orbital ground state, the method of Abragam and Pryce[18,19] may be applied in calculating the g shifts. The g tensor is given by

$$g_{ij} = 2(\delta_{ij} - \lambda\Lambda_{ij}) \quad , \tag{3}$$

where λ is the spin-orbit coupling parameter and

$$\Lambda_{ij} = \sum_{n \neq 0} \frac{\langle 0|L_i|n\rangle\langle n|L_j|0\rangle}{\Delta_n} \tag{4}$$

with $\Delta_n = E_n - E_0$ representing the energy separation to excited states.

Our experimental results indicate that the g tensor has cylindrical symmetry about the F_2^- axis ($\langle 100\rangle$ direction) with $g_\perp > g_\parallel$. The calculation of g values can be simplified by classifying the orbital angular momentum operators according to the irreducible representations of C_{2v}. $(L_x - L_y)/\sqrt{2}$, $(L_x + L_y)/\sqrt{2}$, and L_z transform, respectively, as the Γ_4, Γ_3, and Γ_2 representations of C_{2v} and will therefore couple to the excited states Γ_1, Γ_2, and Γ_3, respectively. In Fig. 9, the energy levels and wave functions are shown together with their classification in C_{2v}. These energy levels have been drawn to be consistent with the observed g shifts.

Equations (3) and (4) may be applied to yield the following results:

$$\Lambda_\perp = \Lambda_{11}$$

$$\cong \frac{|\langle \alpha_{1a}\sqrt{3}xy\,|(L_x - L_y)/\sqrt{2}\,|\,\alpha_4(\sqrt{\tfrac{3}{2}})(xz+yz)\rangle|^2}{\Delta_{1a}}$$

$$= \alpha_{1a}^2\alpha_4^2/\Delta_{1a} \tag{5a}$$

and $g_\perp = g_1 = 2(1 - \lambda\alpha_{1a}^2\alpha_4^2/\Delta_1)$,

$$\Lambda_\perp = \Lambda_{22}$$

$$= \frac{|\langle \alpha_2(\sqrt{\tfrac{3}{2}})(x^2-y^2)\,|(L_x + L_y)/\sqrt{2}\,|\,\alpha_4(\sqrt{\tfrac{3}{2}})(xz+yz)\rangle|^2}{\Delta_2}$$

$$= \alpha_2^2\alpha_4^2/\Delta_2 \tag{5b}$$

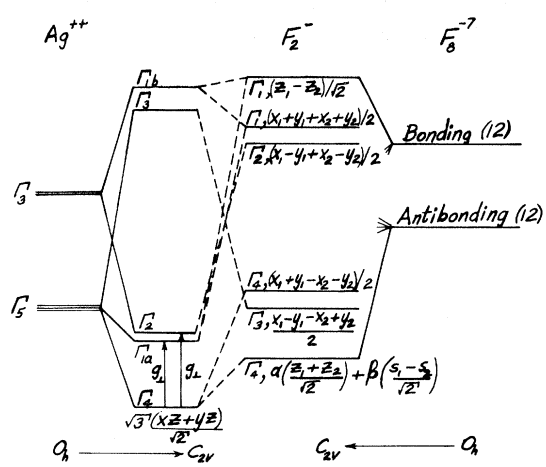

FIG. 9. Energy levels and the wave functions classified according to the C_{2v} symmetry of the distorted configuration. The positioning of the energy levels is drawn to be consistent with the observed g values.

and $g_\perp = g_2 = 2(1 - \lambda\alpha_2^2\alpha_4^2/\Delta_2)$,

$$\Lambda_\parallel = \Lambda_{33} = \frac{|\langle\alpha_3(\sqrt{\tfrac{3}{2}})(xz - yz)|L_z|\alpha_4(\sqrt{\tfrac{3}{2}})(xz + yz)\rangle|^2}{\Delta_3} = \alpha_3^2\alpha_4^2/\Delta_3 \ , \tag{5c}$$

and $g_\parallel = g_3 = 2(1 - \lambda\alpha_3^2\alpha_4^2/\Delta_3)$.

A term involving coupling to the Γ_{1b} state has been neglected. In the above formulas, the α_n's are the probability amplitudes of the ground and excited states on the central ion and are less than one because of the covalent interaction with the fluorines. The subscript n on the α_n's refers to the wave function associated with the represention Γ_n. Values of the experimentally measured g shifts can be used to partially determine some of the parameters. EPR methods can only be used to evaluate the covalent mixing parameters for the ground state. Covalency in the excited states can not be determined directly. Nevertheless, we use the atomic spin-orbit coupling constant of -1840 cm^{-1} for silver[20] to calculate the following parameters:

$$\frac{\Delta_2}{\alpha_2^2\alpha_4^2} \cong \frac{\Delta_{1a}}{\alpha_{1a}^2\alpha_4^2} = 35\,400 \text{ cm}^{-1} \text{ for } CaF_2:Ag^{2+} ,$$
$$\frac{\Delta_2}{\alpha_2^2\alpha_4^2} = \frac{\Delta_{1a}}{\alpha_{1a}^2\alpha_4^2} = 28\,750 \text{ cm}^{-1} \text{ for } SrF_2:Ag^{2+} . \tag{6}$$

The shift in $g_\parallel$ has the wrong sign to agree with Eq. (5c) so we cannot use Eq. (5c) to calculate Δ_3 but we can say that $\Delta_3 \gg \Delta_{1a}$ or Δ_2. To get agreement with the absorption in $CaF_2:Ag^{2+}$ at 25 550 cm^{-1} would require that $\alpha_{1a}^2\alpha_4^2 = 0.72$ and for the 19 000-cm^{-1} peak, $\alpha_{1a}^2\alpha_4^2 = 0.54$. Later in the analysis of hyperfine interactions we will find that for $CaF_2:Ag^{2+}$ the hole spends 91% of its time on the central ion in the ground state. By doing a simple point-charge calculation with a charge of $0.09e$ transferred to the F_2^- the amount of p state mixed in to the ground state is 0.30%. From this result, our estimate for α_4^2 remains about 91%.

The Γ_{1a} excited state at energy Δ_{1a} above the ground state may have somewhat stronger mixing with the fluorine states because of the smaller energy denominators. In fact, if we associate the 25 550-cm^{-1} absorption peak with the $\Gamma_4 \to \Gamma_{1a}$ transition, a value of $\alpha_{1a}^2 = 0.79$ is obtained for $CaF_2:Ag^{2+}$. The other value of $\alpha_{1a}^2\alpha_4^2$ obtained from the 19 000-cm^{-1} absorption peak would not be as acceptable because of the necessarily large covalency required.

In order to calculate $g_\parallel$ we must go to third-order perturbation theory with the spin-orbit interaction as the perturbation. If we neglect the mixing with the Γ_{1b} state and the third-order terms that have Δ_3 in the energy denominator, the new ground-state wave function may be written as follows:

$$\begin{aligned}|\Gamma_4'\rangle = |\Gamma_4\rangle &- \lambda\frac{\langle\Gamma_{1a}|\vec{L}\cdot\vec{S}|\Gamma_4\rangle}{\Delta_{1a}}|\Gamma_{1a}\rangle \\ &- \lambda\frac{\langle\Gamma_2|\vec{L}\cdot\vec{S}|\Gamma_4\rangle}{\Delta_2}|\Gamma_2\rangle - \lambda\frac{\langle\Gamma_3|\vec{L}\cdot\vec{S}|\Gamma_4\rangle}{\Delta_3}|\Gamma_3\rangle \\ &+ \lambda^2\frac{\langle\Gamma_2|\vec{L}\cdot\vec{S}|\Gamma_{1a}\rangle\langle\Gamma_{1a}|\vec{L}\cdot\vec{S}|\Gamma_4\rangle}{\Delta_{1a}\Delta_2}|\Gamma_2\rangle \\ &+ \lambda^2\frac{\langle\Gamma_{1a}|\vec{L}\cdot\vec{S}|\Gamma_2\rangle\langle\Gamma_2|\vec{L}\cdot\vec{S}|\Gamma_4\rangle}{\Delta_{1a}\Delta_2}|\Gamma_{1a}\rangle \ .\end{aligned} \tag{7}$$

The application of this wave function with proper normalization yields an equation for $g_\parallel$,

$$g_\parallel \cong 2.0023 - 2\frac{\alpha_3^2\alpha_4^2\lambda}{\Delta_3} - 2\frac{\alpha_{1a}^2\alpha_2^2\alpha_4^2\lambda^2}{\Delta_{1a}\Delta_2} \ . \tag{8}$$

From the experiment we found that Δ_3 was large compared to Δ_{1a} and Δ_2. Let us assume that it is large enough for the third-order term in Eq. (8) to dominate over the second term on the right. We then calculate the following shifts for $CaF_2:Ag^{2+}$ and $SrF_2:Ag^{2+}$:

$$\Delta g_\parallel = g_\parallel - 2.0023 = -0.0059 \text{ for } CaF_2:Ag^{2+} ,$$
$$\Delta g_\parallel = g_\parallel - 2.0023 = -0.0085 \text{ for } SrF_2:Ag^{2+} . \tag{9}$$

These results are to be compared with the experimental shifts of -0.0053 ± 0.001 and -0.0143 ± 0.001 for Ag^{2+} in CaF_2 and SrF_2, respectively. For SrF_2, the departure from theory is significant.

B. Hyperfine Interactions

The hyperfine interactions are calculated by finding the expectation value of the operator[21]

$$H^{\text{hfs}} = g\frac{\beta\mu_I}{I} \times \sum_i \left[\frac{3(\vec{S}\cdot\vec{r}_i)(\vec{I}_i\cdot\vec{r}_i) - r_i^2(\vec{S}\cdot\vec{I}_i)}{r_i^5} + \frac{8\pi}{3}\vec{I}_i\cdot\vec{S}\,\delta(\vec{r}_i)\right], \tag{10}$$

where g is the electron gyromagnetic ratio, β is the Bohr magneton, μ_I is the magnetic moment of the fluorine nuclei, $\vec{I}_i$ is the spin of one of the fluorine nuclei, and $\vec{r}_i$ is the position of the nucleus. Dipolar interactions between the electrons and the fluorine nuclei are included in the first term. The second term containing the δ function is the Fermi contact interaction which is important when the electrons spend some time in fluorine s states or when there is a depairing of spins in the core s states. Hyperfine interactions with the silver nucleus have not been observed experimentally and we are not including that interaction here. It should be noted that the silver hyper-

fine interactions are never large because the nuclear moment is small. Later we will see that symmetry requires that the wave function have a node through the silver nucleus.

Equation (2) gives the form of the wave function except that smaller terms giving the coupling to fluorines 3, 4, 5, and 6 should be added. In Fig. 8, the wave function is illustrated and the numbering of the fluorines is shown. Our experiment indicates that the probability density on fluorines 7 and 8 is negligible:

$$|\Gamma_4\rangle = \alpha_4(\sqrt{\tfrac{3}{2}})(xz+yz)+\beta_4 z+\gamma_4(z_1+z_2)/\sqrt{2} + \delta_4(s_1-s_2)/\sqrt{2}+\tfrac{1}{2}\epsilon_4(x_1+y_1-x_2-y_2) + \tfrac{1}{2}\zeta_4(y_3+x_5-y_4-x_6)+\tfrac{1}{2}\eta_4(s_3+s_5-s_4-s_6) \quad . \tag{11}$$

This wave function is constructed so that all of the component wave functions transform according to the Γ_4 representation of C_{2v}. After carrying out the calculation the hyperfine Hamiltonian is determined to be as follows:

$$H^{\text{hfs}} = a_1\vec{I}\cdot\vec{S}+d_1(-\vec{I}\cdot\vec{S}+3I_zS_z) + d_2\left(-\vec{I}\cdot\vec{S}+3\frac{(I_x+I_y)}{\sqrt{2}}\frac{(S_x+S_y)}{\sqrt{2}}\right)+a_3\vec{I}'\cdot\vec{S} + d_3\{-\vec{I}'\cdot S+3[(I_{3y}+I_{4y})S_y+(I_{5x}+I_{6x})S_x]\} \quad , \tag{12a}$$

where $\vec{I}=\vec{I}_1+\vec{I}_2$,

$$\vec{I}'=\vec{I}_3+\vec{I}_4+\vec{I}_5+\vec{I}_6 \quad ,$$

$$a_1=\frac{8\pi\mu_I g\beta}{6I}\,|\psi(0)|^2\delta_4^2 \quad ,$$

$$a_3=\frac{8\pi\mu_I g\beta}{12I}\,|\psi(0)|^2\eta_4^2 \quad ,$$

and the d's are coefficients for the dipole-dipole terms,

$$d_1=(\mu_I g\beta/5I)\langle 1/r^3\rangle\gamma_4^2 \quad ,$$
$$d_2=(\mu_I g\beta/5I)\langle 1/r^3\rangle\epsilon_4^2 \quad , \tag{12b}$$
$$d_3=(\mu_I g\beta/10I)\langle 1/r^3\rangle\zeta_4^2 \quad .$$

The hyperfine interactions with the pairs of equivalent fluorines have cylindrical symmetry about $\langle 100\rangle$ axes so the coefficient d_2 must be zero to be consistent with this observed fact. By comparing our hyperfine Hamiltonian to the experimental parameters we derive the values of the parameters in the wave function. This is facilitated by the following relationships:

$$a_1=\tfrac{1}{3}(A_{\parallel}+2A_{\perp}) \quad ,$$
$$d_1=\tfrac{1}{3}(A_{\parallel}-A_{\perp}) \quad , \tag{13}$$

and $$\frac{a_1}{d_1}=\frac{20\pi}{3}\,\frac{|\psi(0)|^2}{\langle 1/r^3\rangle}\,\frac{\delta_4^2}{\gamma_4^2} \quad .$$

Castner and Känzig[16] have analyzed the hyperfine interactions for the F_2^- center and we make use of some parameters given in their paper. They use a value of $\langle 1/r^3\rangle = 60\times 10^{24}\ \text{cm}^{-3}$ that was calculated by Sternheimer for fluorine. Also they estimate a value of $|\psi(0)|^2 = 3.32\times 10^{-24}\ \text{cm}^{-3}$. By employing these calculated values and our experimental parameters we calculate δ_4^2/γ_4^2 for these two cases.

For $CaF_2:Ag^{2+}$,

(a) $A_\perp > 0$: $\delta_4^2/\gamma_4^2 = 1.66$ or 38% p character, 62% S character and $a_1 = 30.8$ G, $d_1 = 16.0$ G;

(b) $A_\perp < 0$: $\delta_4^2/\gamma_4^2 = 0.37$ or 73% p character, 27% S character and $a_1 = 11.1$ G, $d_1 = 25.9$ G.

For $SrF_2:Ag^{2+}$,

(a) $A_\perp > 0$: $\delta_4^2/\gamma_4^2 = 2.97$ or 25% p character, 75% S character and $a_1 = 20.8$ G, $d_1 = 6.0$ G;

(b) $A_\perp < 0$: $\delta_4^2/\gamma_4^2 = 0.06$ or 94% p character, 6% S character and $a_1 = 1.1$ G, $d_1 = 15.9$ G.

Case (b) is the more plausible choice because the wave function on the fluorines should have predominantly p character and becomes more s-like when the hole spends more time on the fluorines.

At this point we want to make an absolute determination of the fluorine wave functions. To do this we compare our data with the hyperfine interactions for F_2^- in CaF_2. For the F_2^- center in CaF_2 we calculate the following parameters from the data of Sierro[15]:

$$a_1 = 267.6\ \text{G}, \quad d_1 = 316.1\ \text{G}.$$

By applying the analysis associated with Eq. (13) we find that the F_2^- wave function has 58% p character and 42% s character. We can calculate the absolute probability densities on the fluorines for $CaF_2:Ag^{2+}$ and $SrF_2:Ag^{2+}$ by multiplying the F_2^- probability density by the ratio of the hyperfine parameters. As an example we calculate δ_4^2 for $CaF_2:Ag^{2+}$ and list other results:

$$\delta_4^2 = 0.42(a_1)_{Ag^{2+}}/(a_1)_{F_2^-} = 0.02 \quad ,$$

$$\gamma_4^2 = 0.05, \quad \text{and } \zeta_4^2 = 0.02 \quad .$$

For $SrF_2:Ag^{2+}$, $\delta_4^2 = 0.002$, $\gamma_4^2 = 0.03$. From these results we can calculate that the hole spends 91% of its time on the central silver ion for $CaF_2:Ag^{2+}$ and 97% of the time for $SrF_2:Ag^{2+}$.

V. DISCUSSION

From the experiment we see that the distortion causes the silver ion and surrounding fluorine ions to shift so that the silver ion has the greatest hyperfine contact with a pair of fluorine ions rather than with all eight. As a result the symmetry is reduced from O_h to C_{2v}. If the Γ_5^+ mode of distortion were strongest we would expect to have trigonal symmetry and a dominant hyperfine inter-

action with pairs of fluorines having orientations along ⟨111⟩ directions rather than in ⟨100⟩ directions as in our experiment. Only an odd mode of distortion such as the Γ_4^- mode can cause the complex to distort in a ⟨110⟩ direction and thereby place a greater hole concentration on pairs of fluorines oriented in ⟨100⟩ directions. In the following paper, we will follow up this line of thought and use a model in which the Γ_4^- mode of distortion plays a key role.

Ions in crystals can also distort for reasons other than electron degeneracy. When a substitutional ion has an ionic radius which is smaller than the ion that would otherwise occupy a lattice site, a distortion may take place.[22] Over the past few years a good deal of interest has been shown in the distortions of Li^+, CN^-, and OH^- ions in alkali halide crystals. Sodium ions do not distort in KCl crystals but Li^+ does distort in ⟨111⟩ directions. The substitutional ion must be a certain critical size smaller than the ion being replaced. We might question whether or not the divalent silver ion distorts because of the size of the ion. Unfortunately the radius of divalent silver is not known very precisely. By extrapolating from the radii of other nearby ions one projects a radius very close to that of Ca^{2+}. For this reason we tend to discount the possibility of distortions associated with small ionic size. One should also note that all of the observed distortions of small ions such as Li^+ have been in ⟨100⟩ and ⟨111⟩ directions but never in ⟨110⟩ directions.

---

[1]H. A. Jahn and E. Teller, Phys. Rev. 49, 874 (1936); Proc. Roy. Soc. (London) A161, 220 (1937); J. H. Van Vleck, Phys. Rev. 52, 246 (1937).

[2]I. B. Bersuker, Zh. Eksperim. i Teor. Fiz. 43, 1315 (1962); 44, 1239 (1963) [Soviet Phys. JETP 16, 933 (1963); 17, 836 (1963)]; Fiz. Tverd. Tela 7, 1231 (1965) [Soviet Phys. Solid State 7, 986 (1965)].

[3]F. S. Ham, Phys. Rev. 138, A1712 (1965); 166, 307 (1968).

[4]M. C. M. O'Brien, Proc. Roy. Soc. (London) A281, 323 (1964); Proc. Phys. Soc. (London) 86, 847 (1965).

[5]U. Opik and M. H. L. Pryce, Proc. Roy. Soc. (London) A238, 425 (1957); H. C. Longuet-Higgins, U. Opik, M. H. L. Pryce, and R. A. Sack, *ibid.* A244, 1 (1958).

[6]R. E. Coffmann, Phys. Letters 19, 475 (1965); 21, 381 (1966); J. Chem. Phys. 48, 609 (1968).

[7]U. T. Höchli, Bull. Am. Phys. Soc. 11, 203 (1966); Phys. Rev. 162, 262 (1967).

[8]F. S. Ham, in *Electron Paramagnetic Resonance*, edited by S. Geschwind (Plenum, New York, 1969).

[9]M. D. Sturge, in *Solid State Physics*, edited by F. Seitz, D. Turnbull, and H. Ehrenreich (Academic, New York, 1967), Vol. 20.

[10]T. L. Estle, G. K. Walters, and M. deWitt, in *Paramagnetic Resonance*, edited by W. Low (Academic, New York, 1963), Vol. 1, p. 144.

[11]K. Morigaki, J. Phys. Soc. Japan, 19, 187 (1964).

[12]R. C. Fedder, Bull. Am. Phys. Soc. 14, 62 (1969), preliminary account of present paper; D. C. Von Hoene and R. C. Fedder, *ibid.* 14, 270 (1969), CdF_2:Ag^{2+}; 14, 48 (1969), CdF_2 : Cu^{2+}; see also Phys. Letters 30, 1 (1969).

[13]W. Kanzig, Phys. Rev. 99, 1890 (1955).

[14]W. Hayes and J. Twidell, Proc. Phys. Soc. (London) 79, 1295 (1962).

[15]J. Sierro, Phys. Rev. 138, A648 (1965).

[16]T. G. Castner and W. Kanzig, J. Phys. Chem. Solids 3, 178 (1957). The experiments of Hayes and Twidell, Ref. 14, show that the electronic properties of the V_k center in CaF_2 are almost identical to those in LiF.

[17]G. F. Koster, J. O. Dimmock, R. G. Wheeler, and H. Statz, *Properties of the Thirty-Two Point Groups* (MIT Press, Cambridge, Mass., 1963). Their notation is used throughout this paper.

[18]An alternative would be to calculate the g value for the orbital Γ_5^+ triplet state. The reader is referred to M. Kotani [J. Phys. Soc. Japan 4, 293 (1949)], where the g value is calculated to be precisely 2.00 for the Γ_7 level and approximately zero for the Γ_8 level. One expects the Γ_7 level to be lowest in energy for the $4d^9$ configuration of Ag^{2+} in CaF_2. The inclusion of mixing between the two Γ_8 states that arise from the orbital triplet and doublet levels will not alter the g values of the Γ_7 level. For this reason and because of the internal consistency of our results we believe that the ground state is an orbital singlet.

[19]A. Abragam and M. H. L. Pryce, Proc. Phys. Soc. (London) A63, 409 (1950).

[20]K. D. Bowers, Proc. Phys. Soc. (London) A66, 666 (1953); W. P. Gilbert, Phys. Rev. 48, 338 (1935).

[21]A. Abragam and M. H. L. Pryce, Proc. Roy. Soc. (London) A205, 135 (1951); C. P. Slichter, *Principles of Magnetic Resonance* (Harper and Row, New York, 1963), pp. 87, 189.

[22]U. Kuhn and F. Luty, Solid State Commun. 2, 281 (1964); M. Gomez, S. P. Bowen, and J. A. Krumhansl, Phys. Rev. 153, 1009 (1967); P. Sauer, O. Schirmer, and I. Schneider, Phys. Status Solidi 16, 79 (1966), and references in these papers.